Effect of Tip Functionalization on Transport through Vertically Oriented Carbon Nanotube Membranes

Mainak Majumder,[†] Nitin Chopra,[†] and Bruce J. Hinds*,[†,‡]

Contribution from the Chemical and Materials Engineering Department, University of Kentucky, Lexington, Kentucky 40506, and Department of Chemistry, University of Kentucky, Lexington, Kentucky 40506

Received November 19, 2004; E-mail: bjhinds@engr.uky.edu

Abstract: Ionic flux through a composite membrane structure, containing vertically aligned carbon nanotubes crossing a polystyrene matrix film, was studied as a function of chemical end groups at the entrance to carbon nanotubes' (CNTs) cores. Plasma oxidation during the membrane fabrication process introduced carboxylic acid groups on the CNTs' tips that were modified using carbodiimide mediated coupling between the carboxylic acid and an accessible amine groups of the functional molecule. Functionalization molecules included straight chain alkanes, anionically charged dye molecules, and an aliphatic amine elongated by polypeptide spacers. Functionalization was confirmed by FTIR spectroscopy, and areal functional density was estimated by transmission electron microscopy studies of thiol terminated sites decorated by nanocrystalline gold. The transport through the membrane of two different sized but equally charged molecules (ruthenium bipyridine [Ru-(bipy)$_3^{2+}$] and methyl viologen [MV^{2+}]) was quantified in a U-tube permeation cell by UV−vis spectroscopy. Relative selectivity of the permeates varied from 1.7 to 3.6 as a function of tip-functionalization chemistry. Anionic charged functional groups sharply increased the flux of the cationic permeates. This effect was reduced at higher solution ionic strength consistent with shorter Debye screening length. The observed selectivities were consistent with a hindered diffusion model with functionalization at the CNT tip and not along the length of the CNT core.

1. Introduction

Synthesis and characterization of ordered nanoporous materials with nontortuous and well controlled pore diameter is an active research area with applications that include separations, catalysis, molecular sensing, and controlled drug delivery.[1−3] Synthesis of a suitable membrane structure with a highly ordered vertical orientation of pores is a difficult challenge.[4,5] A promising approach for obtaining a vertically oriented membrane structure has been the controlled reduction of pore size of existing ordered porous structures such as anodized alumina or track etch polycarbonate membranes.[6] A flurry of research activity for reducing pore size by electroless deposition[7] or CVD[6,8] has demonstrated improvement in O$_2$/N$_2$ and water vapor/oxygen separation coefficients. Critical to membrane separations is fine control of pore size with high uniformity. The inner core of carbon nanotubes (CNTs) offer an alternative route to uniform membrane pore diameter with fine control

determined by catalytic particle size.[9] Of interest are the transport mechanisms of gaseous[10] and liquid molecules[11,12] through the graphitic cores of the CNTs. There is a need for further experimental verification of theoretical studies. Transport studies of polystyrene particles in an aqueous medium through a single carbon nanotube (100 nm diameter) membrane[13] and ionic transport through carbon plated porous alumina[14] indicate the ability for aqueous systems to function in carbon systems. This led to interest in studying transport through cores with dimensions less than 10 nm and having the smoothness inherent to graphitic carbon nanotubes. Recently, vertically aligned carbon nanotube membranes with CNT cores (∼7 nm diameter) traversing across a thin solid polymer film were synthesized.[15] Ionic and gas transport through the CNT membrane were seen to be consistent with the observed areal density of aligned CNT cores. Generally, functional molecules attached to the pore surfaces can also lead to highly selective separations by forcing a chemical interaction between the permeate and the functional

[†] Chemical and Materials Engineering Department.

[‡] Department of Chemistry.

(1) Davis, M. E. *Nature* **1993**, *364*, 391.
(2) Steinle, E. D.; Mitchell, D. T.; Wirtz, M.; Lee, S.B; Young, V. V.; Martin, C. R. *Anal. Chem.* **2002**, *74*, 2416−2422.
(3) Martin, C. R.; Kohli, *Nature* **2003**, *2*, 29−37.
(4) Brinker, C. J.; Lu, Y.; Sellinger, A.; Fan, H. *Adv. Mater.* **1999**, *11*, 579−585.
(5) Tolbert, S. H.; Firouzi, A.; Stucky, G. D.; Chemlka, B. D. *Science* **1997**, *278*, 264−267.
(6) Jirage, K. B.; Hulteen, J. C.; Martin, C. R. *Science* **1997**, *278*, 655−658.
(7) Hulteen, J. C.; Martin, C. R. *J. Mater. Chem.* **1997**, *7*, 1075−1087.
(8) Alsyouri, H. M.; Langheinrich, C.; Lin, Y. S.; Ye, Z.;. Zu, S. *Langmuir* **2003**, *19*, 7307−7314.

(9) Cheung, C. L.; Kurtz, H. P.; Leiber, C. M. *J. Phys. Chem. B* **2002**, *106*, 2429−2433.
(10) Mao, Z.; Sinnot, S. *Phys. Rev. Lett.* **2002**, *89*, 278301-1-4.
(11) Hummer, G.; Rasaih, J. C.; Nowortya, J. P. *Nature* **2001**, *414*, 188−190.
(12) Kalra, A.; Garde, S.; Hummer, H. *Proc. Natl. Acad. Sci.* **2003**, *100*, 10175−10180.
(13) Sun, L.; Crooks, R. M. *J. Am. Chem. Soc.* **2000**, *122*, 12340−12345.
(14) Miller, S. A.; Young, V. Y.; Martin, C. R. *J. Am. Chem. Soc.* **2001**, *123*, 12335−12342.
(15) Hinds, B. J.; Chopra, N.; Rantell, T.; Andrews, R.; Gavalas, V.; Bachas, L. *Science* **2004**, *303*, 62−65.

molecule.[16−18] Since the oxidation process to fabricate CNT membranes selectively functionalizes the entrances/tips of CNT cores, this system offers a unique nanoscale scaffolding to permit "gatekeeper" chemical interactions. This approach has the possibility to increase both flux and selectivity of separation processes. With proper functionality, transport through hydrophobic CNT cores would be analogous to biological membrane channels. Studies of biological membrane systems are filled with examples where protein molecules facilitate the transport of ions or molecules.[19] The opening of gated ion channels are determined by voltage dependent movements of charged arginine residues within membrane pores.[20] This could possibly be mimicked by voltage applied to conductive CNTs. Recently, there have been studies of the transport of water and electrolyte (KCl) through CNTs using molecular dynamic simulations. These have predicted that the charge state of carboxylate groups at the entrance to the CNT cores significantly enhances the incorporation of ions into the CNT core.[21] Motivation for this present study stems from biological systems, in which protein molecules regulate the transport properties of ions across hydrophobic regions of micelle membranes.

The CNT membranes are an interesting membrane structure with a large areal density of graphitic cores having entrances that can be functionalized by molecules of desired length, hydrophilicity, or chemical functionality. Since the tips are functionalized with carboxylate groups from an oxidative CNT cutting step, simple carbodiimide chemistry can be performed with desired functional molecules containing accessible amine. These functional molecules can be utilized to investigate a "gatekeeper" mechanism for controlling the flow and selectivity of chemical transport through the CNT membranes. Of particular interest for initial studies is the effect of the CNT-functional molecule size, hydrophilicity, and charge on the flux and the relative selectivity of two similarly charged but differently sized permeate molecules through the CNT membranes. This paper presents the experimental procedures for the chemical functionalization of CNT membranes. Functionalization was confirmed by FTIR spectroscopy, and the areal functional density was estimated by transmission electron microscopy studies of thiol terminated sites decorated by nanocrystalline gold. Diffusive mass transport of two similarly charged but differently sized molecules through the CNT membranes demonstrated that chain length, solubility/conformation, charge of the functional molecule, and solution ionic strength affected the flux and selectivity of the permeate molecules. The selectivity data were then analyzed using hindered diffusion models to demonstrate that selective transport occurred near the CNT tip entrances and not along the entire length of the CNT, consistent with a "gatekeeper" geometry.

2. Experimental Section

2.1. Membrane Fabrication. CNT membranes were fabricated using the previously described method which is briefly summarized here.[15]

An aligned array of multiwalled CNTs was grown by chemical vapor deposition (CVD) using ferrocene/xylene feed gas. The volume between CNTs was filled with polystyrene (without disrupting initial alignment), and the composite film was removed from the quartz substrate by HF etching. Excess surface polymer and Fe nanocrystals at the tips of the CNTs were removed by H_2O plasma oxidation.[22] This resulted in a membrane structure with CNT cores transversing the polystyrene film and carboxylate functionalization at the CNT tips.

2.2. Functionalization. CNT membranes were functionalized using conventional carbodiimide chemistry. The following chemicals were used: 1-[3-(dimethylamino)propyl]-3-ethylcarbodiimide hydrochloride (EDC,98%,Aldrich), nonylamine (C9,98%, Aldrich), Direct Blue 71 (dye, Aldrich), 8-amino caprylic acid (ACA,99%,Aldrich), Kemamine P-298D, (C22, Crompton Corporation, USA), 2-*N*-morphilino ethanesulfonic acid (MES, 99%, Sigma), isopropyl alcohol (99.5%, EMD), ethyl alcohol (Aaper Alcohol and Chemical Co., Kentucky). For reactions in water, deionized (DI) water (∼18 mΩ resistance) was used. The functional molecules are shown in Figure 1.

For the water soluble functional molecules (C9 and dye), 8 mg of EDC were dissolved into 4 mL of 50 mM aqueous solution of the functional molecule in 0.1 M MES buffer. The membrane was added to the solution for 12 h at ambient temperature, after which the membrane was washed with MES buffer and IPA to remove the excess reagents. The functionalized membranes will henceforth be referred to as CNT-C9 and CNT-dye.

For water insoluble functional molecules, Kemamine is a commercial fatty amine containing about 90% C22. It is insoluble in water but soluble in IPA at 35° C. EDC based coupling reactions were earlier carried out in an alcohol medium.[23] C22 (32.36 mg) and EDC (8 mg) were added to 4 mL of IPA along with the membrane, kept in a water bath at 35° C for 12 h, and then washed with ethyl alcohol. The functionalized membrane will henceforth be referred to as CNT-C22.

For ACA functionalization, the membrane was first surface activated in 4 mL of 0.1 M MES by 8 mg of EDC, and the membrane was then placed into a 50 mM solution of ACA in 0.1 M MES buffer. Functionalization was thus carried out in two steps: (1) activation with terminal COOH groups with EDC and (2) reaction with ACA. This process avoids polymerization of ACA and sequentially adds peptides to the membrane surface. These two reaction steps were repeated 4 times to increase the spacer length, and then the membrane was finally functionalized with C9 using the water soluble method described earlier. The membrane was washed with MES buffer and then with IPA. The functionalized membrane will henceforth be known as CNT-C40 (polypeptide). Tip functionalization molecular length was estimated by minimizing conformational energy using MM_2 routine.

2.3. FTIR Studies. The membrane was dissolved in toluene (Mallinckrodt, 100%) and then centrifuged to remove the polymer. The purified nanotubes in toluene were then mixed with FTIR grade KBr (Sigma-Aldrich, >99%) and dried in a vacuum oven. The dried powder was then examined in a ThermoNicolet Nexus 4700. FTIR spectra were analyzed after subtraction of KBr spectra from each.

2.4. U-Tube Permeation Experiment. A schematic of the U-tube cell is shown in Figure 2. The seal between the membrane and the cell was made with a Vitron O-ring, and the liquids in the two chambers were maintained at the same level to avoid any pressure induced transport. The probe molecules, methyl viologen dichloride hydrate and ruthenium bipyridine hexahydrate, were purchased from Aldrich. The probe molecules were chosen for their ease of detection by UV−vis and for the ability to directly compare fluxes and selectivities with other nanoporous systems.[6] The permeate was periodically pipetted out with the probe molecules readily quantified by UV−vis spectroscopy (HP 8543 spectrophotometer). The permeate was then was transferred back to the chamber. Ru-(bipy)$_3^{2+}$ has two peaks at wavelengths of 452 and

(16) Lee, S. B.; Mitchell, D. T.; Trofin, L.; Nevanen, T. K.; Soderland, H.; Martin, C. R. *Science* **2002**, *296*, 2198−2200.
(17) Randon, J.; Patterson, R. *J. Membr. Sci.* **1997**, *134*, 219−223.
(18) Feng, X.; Fryxell, G. E.; Wang, L.-Q.; Kim, A. Y.; Liu, J.; Kemner, K. M. *Science* **1997**, *276*, 923−926.
(19) Jacobson, G.; Zubay, G. *Biochemistry*, 4th ed.; Wm. C. Brown Publishers.
(20) Jiang, Y.; Ruta, V.; Chen, J.; Lee, A.; Mackinnon, R. *Nature* **2003**, *423*, 42−48.
(21) Joshep, S.; Mashi, R. J.; Jackobsson, E.; Aluru, N. *Nano Lett.* **2003**, *3*, 1399−1403.

(22) Huang, S. M.; Dai, L. M. *J. Phys. Chem. B* **2002**, *106*, 3543−3545.
(23) Liu, Z.; Shen, Z.; Zhu, T.; Hou, S.; Ying, L.; Gu, Z. *Langmuir* **2000**, *16*, 3569−3573.
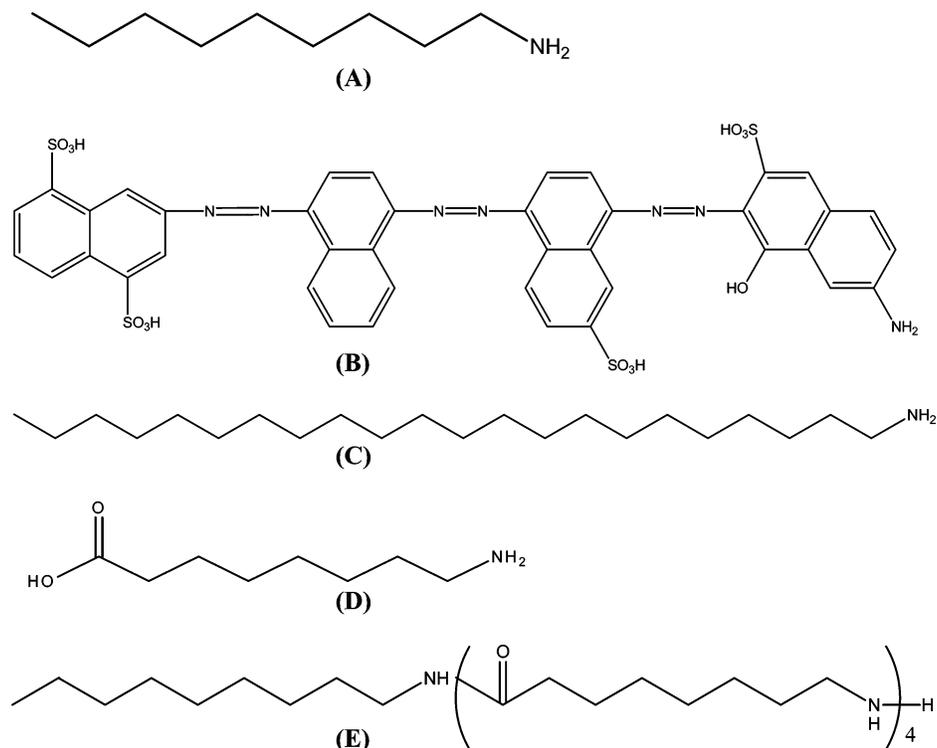
Figure 1. Schematic of the molecules used for functionalizing nanotube membrane (A) C9; (B) dye; (C)C22; (D) ACA; (E) C40 (polypeptide) (formed after four sequential reactions of ACA, followed by C9)
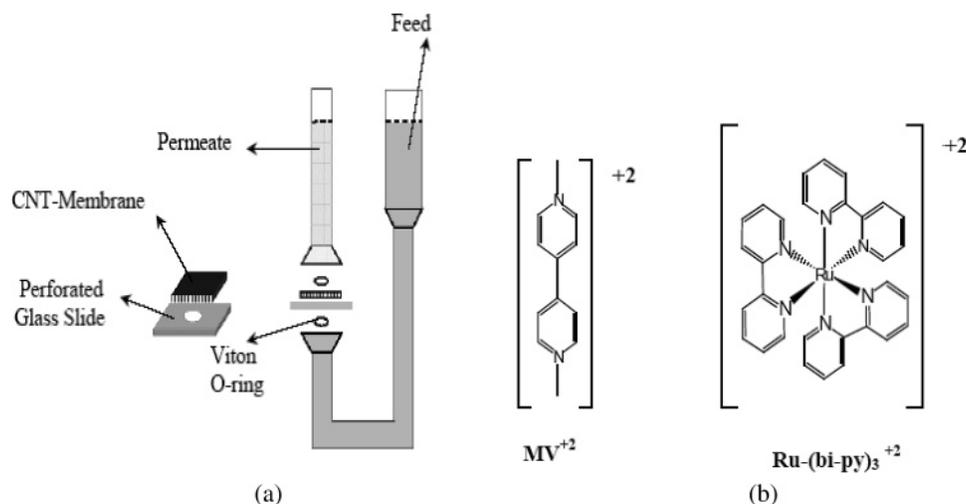
Figure 2. (a) Schematic of the permeation cell. The feed solution is 5 mM in Ru-(bipy)$_3^{2+}$ and 5mM in MV^{2+}, the permeate volume is 1.3 mL, and the exposed membrane area is 0.3 cm^2. (b) The probe molecules have similar charge but different sizes and shapes. Ru-(bipy)$_3^{2+}$ is a spherical molecule of about 11 Å diameter, and MV^{2+} is a cylindrical molecule of 5 Å equivalent spherical diameter (10 Å long, 3 Å diameter).

286 nm, whereas MV^{2+} has a peak at 260 nm. The peak at 452 nm is used to quantify the amount of Ru-(bipy)$_3^{2+}$ without interference from MV^{2+}. To quantify the MV^{2+} peak at 260 nm, the proportional measured Ru-(bipy)$_3^{2+}$ absorbance at 452 nm was subtracted from the absorbance at 260 nm. Six-point calibration curves (from 5×10^{-4} M to 1×10^{-6} M) were used for each analyte.

3. Results and Discussions

3.1. FTIR Spectroscopic Studies. To monitor the functionalization reaction, FTIR spectra of CVD grown as-received CNT, plasma oxidized CNT, CNT-dye, CNT-C9, and CNT-C22 are shown in Figure 3a. The expanded and smoothed view of the region of C=O stretch is shown in Figure 3b.

As received CNTs show minimal C=O stretch. In the case of plasma oxidized CNT, a peak at 1630 cm^{-1} was found. This can be attributed to C=O stretch in carboxylic acid. For chemically oxidized single-walled CNTs (SWCNTs), carbonyl stretch for carboxylic acid groups[24] has been found in the range 1700–1750 cm^{-1}. This was not observed in our case since we used the much larger diameter multiwalled CNTs (MWCNTs). A shift of C=O stretch to lower frequencies can occur with larger aromatic groups.[25] Carbonyl peaks near 1630 cm^{-1} have also been observed near 1635 cm^{-1} in MWCNTs,[26] and our

(24) Basuik, E.; Basuik, A. V.; Banuelos, J. G.; Saniger-Blesa, J. M.;Pokrovskiy, V. A.; Gromovoy, Y.; Mischanchuk, A. V.; Mischanchuk, B. G. *J. Phys. Chem. B* **2002**, *106*, 1588–1597.
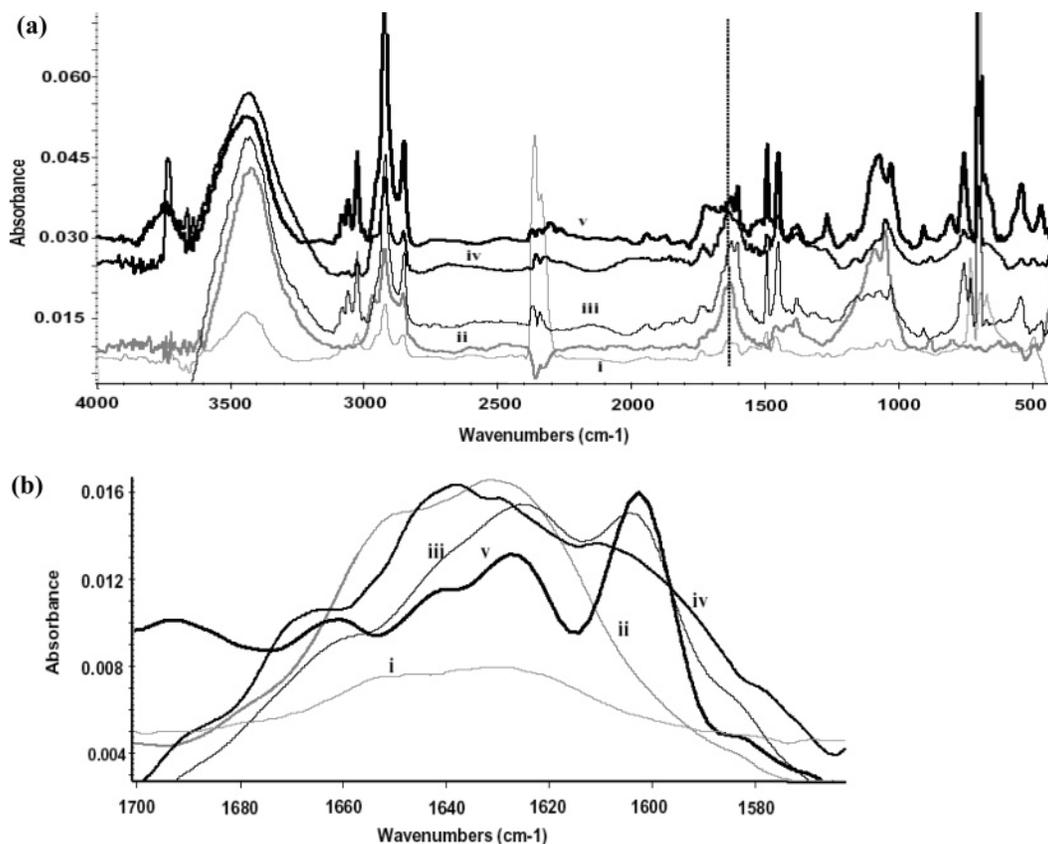
Figure 3. (a) FTIR spectra and (b) expanded and smoothed view of region of C=O stretch. Spectra is identified as (i) as-received CNTs; (ii) plasma oxidized membrane; (iii) CNT-dye; (iv) CNT-C9; and (v) CNT-C22 membrane. The spectra in part a are offset for clarity. The polystyrene matrix of membranes is dissolved in and washed with toluene before forming KBr pellets. The functionalized membranes show amide stretches. Data shown in expanded region are smoothed with an 11-point boxcar routine.

observed shift after carbodiimide functionalization is consistent with carboxylate assignment. Also noticed was OH peak intensity at $3400-3500$ cm^{-1} consistent with carboxylic acid groups, but conclusive interpretation is limited by overlap with peaks of absorbed water in the KBr pellets.

The peaks between 3000 and 3100 cm^{-1} are characteristic of aromatic C—H stretches thus indicating an experimental difficulty of removing all the polystyrene or toluene solvent, adsorbed on or within (toluene) the opened nanotubes. Polystyrene and toluene also have characteristic absorptions at $2850-2950$, 1715, 1600, 1495, 1450, 1270, and 1050 cm^{-1}. Many of the similarities in spectra (iii, iv, and v) can be attributed to residual polystyrene or toluene. Functional molecules would primarily have peaks in the region $2800-3050$ cm^{-1} (C—H stretches) and carbonyl stretches in $1600-1700$ cm^{-1}. In the case of the dye molecule, aromatic peaks overlapping with polystyrene/toluene would also be expected. The expanded view of the region of C=O stretch for the functionalized membranes showed that the peak had broadened with the maximum at 1630 cm^{-1} and a shoulder at 1600 cm^{-1} (for CNT-dye) and 1604 cm^{-1} (for CNT-C9) whose intensity is less than the peak at 1630 cm^{-1}. These peaks can be assigned amide (I) and amide (II) bands, respectively.[23] However for CNT-C22, a sharp peak at 1600 cm^{-1} is observed. Both the intensity and location of amide (I) and amide (II) stretches can be dependent on the local chemical environment. For instance, lower hydrogen bonding lengths (higher hydrophobicity) have been found to shift amide (I) stretches to lower frequencies in proteins.[27] In our case the presence of the highly hydrophobic environment of CNT-C22 (in a conformation absorbed along the wall of CNT, consistent with following transport studies) may shift the amide (I) stretch to lower frequency, resulting in the sharp peak at 1600 cm^{-1}. However interference from residual polystyrene or toluene (C—C aromatic stretch at 1600 cm^{-1}) makes this line of analysis inconclusive.

3.2. Effect of Functional Molecule Chain Length on Ionic Flux and Selectivity through CNT Membrane. Measurement of the transport of molecules through a porous material is an effective method of probing the size and chemical state of pore interiors.[28] Hindered diffusion occurs in pores when the size of the permeating species is large enough to force significant interaction with the pore walls.[29] The transport of two molecules having similar charge but different size (Ru-(bipy)$_3$$^{2+}$ and MV^{2+}) can show the relative hindrance provided by functional molecules at the entrance of the CNT cores. The summary of the transport properties through the membranes as a function of chemical functionalization is shown in Table 1. Figure 4 shows a representative plot of the transport of Ru-(bipy)$_3$$^{2+}$ and MV^{2+} through the membrane as a function of time.

(25) Pavia, D.L.; Lampman, V.; Kriz, S. G. In *Introduction to Organic Laboratory Techniques-contemporary approach*, Appendix 3, 2nd ed.; Saunders College Publishing.
(26) Liu, Y. Q.; Gao, L. *Carbon* **2005**, *43*, 47−52.
(27) Reisdorf, W. C.; Krimm S. Infrared Amide I Band of the Coiled Coil. *Biochemistry* **1996**, *35*, 1383−1386.
(28) Bath, B. D.; White, H. S.; Scott, E. R. *Anal. Chem.* **2000**, *72*, 433−442.
(29) Kathawala, I. A.; Anderson, J. L.; Lindsey, J. A. *Macromolecules* **1989**, *22*, 1215−1218.

Table 1. Summary of Transport Measurements Across CNT Membranes (0.3 cm^2 Area, 5 mmol of Each Source) from a Two-Component Source Solution[a]

membrane tip functionality	size of molecule (Å)	MV^{2+} flux (nmol/h) (90% confidence)	Ru-(bipy)$_3{}^{2+}$ flux (nmol/h) (90% confidence)	α	pore size calcd from α (Å)
CNT	0	4.21 (±1.0)	2.45 (±0.39)	1.7	67
CNT-C9	11.4	6.40 (±2.18)	2.12 (±0.90)	3.0	37
CNT-dye	26	21.05 (±2.32)	9.57 (±0.91)	2.2	47
CNT-C22	28	1.84 (±0.48)	0.93 (±0.22)	2.0	50
CNT-C40	52	0.65 (±0.13)	0.18 (±0.02)	3.6	33

[a] Simultaneous flux of permeate is calculated from the linear fit of solute concentration vs time. The separation factor (α) was experimentally measured for the membranes. Pore size was calculated from the observed separation factor (α) and using a hindered diffusion model of functionalization at the CNT entrance (model (i)).
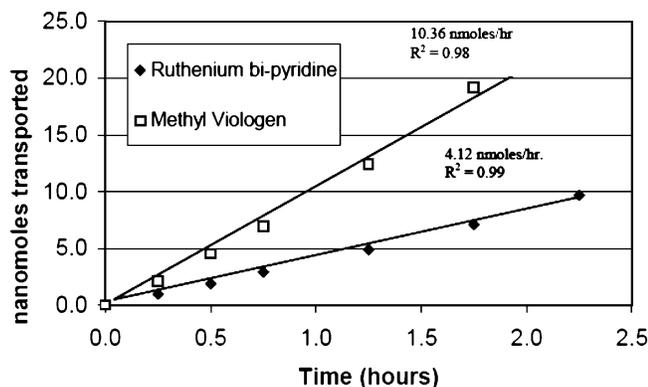
Figure 4. Representative plot of Ru-(bipy)$_3{}^{2+}$ and MV^{2+} transport through CNT-dye membrane in 0.1 M KCl. Separation factor (α) is the ratio of the slopes of the linear fit of flux with time.

The UV−vis measurements were not carried out in situ. Specifically, they were not made continuously using the U-tube as a UV−vis cell. Instead, the flux experiment was interrupted to analyze the entire volume of the analyte cell. Due to time constraints of sequential analysis, each flux series (Figure 4) has only 6 or 7 data points. This increases the amount of uncertainty in predicting the flux rates (slope of linear fit) from the measured values. Along with the mean sample transport rate, we showed the (±) uncertainty at the 90% confidence level. We used the equation $ts/n^{0.5}$ where n is the number of observations, t is the student's t value at $n − 1$ degrees of freedom, and s is the standard deviation of the measured values from the linear fit.

It is also important to note that the Fe-catalyzed CVD process for synthesizing aligned CNTs can lead to the presence of iron nanoparticles in the CNT cores causing sample-to-sample variation in membrane transport. Plasma oxidation and HCl treatment are used to remove iron particles, but in extreme cases they remain to reduce the absolute flux values. As a control experiment, we made "membranes" using identical process steps (and thickness) from regions of the deposition reactor where all CNTs are blocked by Fe. No flux (either MV^{2+} or Ru-(bipy)$_3{}^{2+}$) was detected, even after 3 days of diffusion experiments. The detection limit of the instrument was 5.15×10^{-8} M for Ru-(bipy)$_3{}^{2+}$. Using a cell volume of 1.3 mL, the detection limit of this cell is 0.009 nmol/h. This indicated that diffusion through or defects in polystyrene polymer film were not significant transport mechanisms. The selectivities (α, the ratio of the transport rates of the two species) in these

simultaneous flux experiments would not be affected by any CNTs that were blocked by Fe.

In general the separation coefficients between MV^{2+} and Ru-(bipy)$_3{}^{2+}$ were modest (1.7−3.6) compared to porous alumina where separation coefficients were as high as 1500.[6] In the alumina case, pore size reduction was accomplished by solid plating to sizes less than the diameter of Ru-(bipy)$_3{}^{2+}$. In our case, the areal density of the functionalized molecule may not be complete (as it would be in the case of solid pore plating) and the conformation of the molecules may change with solvent conditions. The observed selectivity is consistent with a "gate-keeper" functionality at the CNT tips. In optimized systems, the tip functionality would have the advantage of a short path length of hindered diffusion, thereby increasing overall permeate flux.

From established hindered diffusion studies, an increase in the separation factor would be expected from a decrease in pore size by the attachment of functional molecule. The separation factor for the initial CNT membrane with COOH functionality is α = 1.7. This increases to α = 3 in the CNT-C9 case. Purely geometric arguments using the diameter of the CNT core would give a pore size of 47 Å (7 nm nominal core diameter minus twice the molecule). Pore size reductions by depositing molecules in mesoporous silica materials using silane chemistry have been reported to be consistent with the length of the molecule.[30] However, when a longer aliphatic amine of length ∼28 Å (CNT-C22), was attached to the CNT membrane, the selectivity actually declined to α = 2.0. The Ru-(bipy)$_3{}^{2+}$ flux also decreased compared to that of CNT-C9, by a factor of about 2.2. The overall flux through CNT-C22 was reduced by increased hydrophobicity at the pore entrances. This has also been the case with C$_{18}$ modified porous alumina[2] having very little transport of water and hydrophilic permeates. Liquid permeation experiments in hydrophobic membranes have also shown lower permeability of polar molecules such as water and alcohols as compared to alkanes, while the reverese is true for hydrophilic membranes.[31] Since the separation factor is a function of the pore diameter at the CNT entrances, attachment of a larger molecule should ideally give a reduced pore size as was observed in hydrophilic mesoporous silica (as measured by BET).[29] In all our cases, it is possible that a molecularly dense functionalilty was absent at the CNT core entrance due to a relatively small number of carboxylic acid groups at the CNT tips. This gave a reduced separation coefficient as compared to pore-plating methods. For long-chain alkanes, van der Waals interaction of the chains with the walls of the graphitic CNT core was expected to dominate compared to chain−chain interaction. The reduction of the separation factor in CNT-C22 compared to CNT-C9 was consistent with the long hydrophobic alkyl chains preferring the surface of the hydrophobic CNTs and not protruding out into the aqueous channel. This was in contrast to the case of alumina or silica pores, where the long chain alkane interactions with the pore wall would be relatively weak.

3.3. Effect of Charge and Functional Molecule Aqueous Solubility. Functionalization of the membrane with the anionically charged dye molecule (CNT-dye) led to increased flux of

(30) Liu, J.; Shin, Y.; Nie, Z.; Chang, J. H.; Wang, L. Q.; Fryxell, G. E.; Samuels, W. D.; Exarhos, G. J *J. Phys. Chem. A* **2000**, *104*, 8328−8339.
(31) Bhanushali, D.; Kloos, S.; Kurth, C.; Bhattacharyya, D. *J. Membr. Sci.* **2001**, *199*, 1−21.

Table 2. Transport Measurement Across CNT-Dye in Different Concentrations of Electrolyte (KCl)

electrolyte concn (M) KCl	MV^{2+} flux (nmol/h) (90% confidence)	$Ru\text{-}(bipy)_3{}^{2+}$ flux (nmol/h) (90% confidence)	α
0	21.1 ($\pm$2.3)	9.57 ($\pm$0.91)	2.2
0.01	8.88 ($\pm$0.40)	3.24 ($\pm$0.17)	2.7
0.1	10.36 ($\pm$0.97)	4.12 ($\pm$0.28)	2.5

positively charged species. It increased $\sim$4-fold compared to the unmodified CNT membrane. Potential-dependent transport of charged species was demonstrated in gold nanotubule membranes.[32] $Ru\text{-}(bipy)_3{}^{2+}$ flux increased $\sim$2.8 times in 3.2 nm diameter and $\sim$3.3 times in 1.5 nm gold nanotube membrane when the applied potential was -0.4 V. This was compared to the flux in the membranes without any bias. Comparable increase of flux in CNT-dye indicated that there are electrostatic attractive forces acting on the positively charged permeate species by the negatively charged dye molecule. Along with an increase in flux, an increase of separation factor in CNT-dye compared to CNT-C22 was also observed despite the fact that the dye molecule is slightly smaller than C22. The presence of the charged functional molecule would not lead to an increase in the separation factor based on electrostatic attractions because of the identical charges on MV^{2+} and $Ru(bipy)_3{}^{2+}$. Instead, the increase is due to the conformation of the charged, soluble dye molecule. Molecules in favorable solvents are entropically stable to be in an open position as opposed to a folded one. This contributes to a larger decrease in pore size, which increases the separation factor. Conformational changes of molecules in solvents have been reported to regulate accessibility of microcavities in long chain monolayers formed by molecular imprinting.[30] In CNT-C40, sequential addition of ACA (4 times) was followed by reaction with C9 amine, so that the terminal group was an alkane group and not COOH. The long chain molecule was about 52 Å long with a relatively hydrophilic peptide bond which should geometrically block the pores. Compared to CNT-C22, the CNT-C40 had a decrease in $Ru\text{-}(bipy)_3{}^{+2}$ flux ($\sim$5 times) and an enhancement in the separation factor to $\alpha = 3.6$. Thus, the separation factor could be increased by attaching relatively hydrophilic long chain molecules. In the case of long aliphatic chain lengths (C22) the separation factors do not increase significantly ($\alpha = 2.0$) because the molecules prefer to be oriented along the carbon nanotube walls instead of protruding into the aqueous channel.

3.4. Effect of Solvent Ionic Strength on Transport through CNT-Dye Membrane. By functionalizing the entrance to the CNT core with an anionically charged dye molecule, the flux of cationic permeates dramatically increased. The length of space charge layer (ionic strength of the solution) should affect the flux of the permeates and the separation factor. These observations are shown in Table 2.

There was nearly a 3-fold decrease in $Ru\text{-}(bipy)_3{}^{2+}$ flux when the electrolyte strength increased to 0.01 M KCl. This is consistent with short screening lengths (at high ionic strength) reducing the Coloumbic attraction of the cationic permeate to the anionic functional groups, which reduces the overall flux. A theoretical study[21] of SWCNTs of 2.2 nm diameter found strong enhancement of ionic flux into a CNT core with charged

carboxylate groups. Though the inner core diameters of MWCNTs in this experimental study were about 7 nm, the dye molecules were about 2.6 nm long, resulting in an effective diameter of 1.8 nm (diameter minus twice the functional molecule). This suggests that the length scales between theoretical SWCNT and this experiment are appropriate for comparison. It is unclear if that anionic carboxylate groups of "as-made" membranes ($\sim$7 nm inner diameter) do help cationic flux as compared to neutral entrances. The CNT-C9 membrane would have a neutral charge at the entrance (if completely functionalized) and does not show dramatically reduced cationic flux compared to the as-made CNT membrane. In the case of CNT-C22 a dramatic decrease in flux is seen, which may be due to more efficient functionalization in IPA solvent or increased hydrophobicity. Since the tetravalent dye molecule extends into the core cross section, the CNT-dye membrane appears to have a higher efficiency for cation attraction compared to the "as-made" membrane. The ionic strength of the solution can also alter the wetting of hydrophobic surfaces. A reduced rate of N_2 bubble nucleation and coalescence on hydrophobic surfaces is seen at increasing KCl concentrations.[33] Thus, in the presence of increased electrolytes, the phenomena of air bubbles should result in an increase in the flux of cationic species due to a decrease in air bubbles at hydrophobic CNT surfaces. Our experimental observations are a decreased flux of the cationic species in electrolytic solutions, thus suggesting that electrostatic effects are dominant.

Electrostatic interactions should be equal for divalent cations and should not lead to an increase in selectivity. A modest observed increase in permeate selectivity with increased solvent ionic strength indicated that there was also a pore size reduction. This may be a result of the electrostatic conformation of the dye molecule. An increase in the molecular interaction area in salt solutions due to dipolar coupling between the polar groups and ions has been reported in Langmuir/Langmuir−Blodgett films.[34] Such interaction would be prominent in the charged dye molecule leading to conformational changes with a corresponding decrease in pore size. For a reported flux of a neutral molecule (phenol) through a larger carbon nanotube membrane (120 nm pore diameter),[13] there was not any change in diffusional flux with a change in electrolyte ionic strength. However, they found electroosmotic velocity decreased with increasing ionic strength. In our case there was no applied potential, and thus we would not expect electroosmosis to be significant. This suggests that the conformation of the dye molecule is significant.

3.5. Comparison of Observed Selectivity to Hindered Diffusion Models. Observed separation coefficients between differently sized permeate molecules can give insight into the geometry of the membrane pores. The diffusivity (D_0) of a solute in bulk solution is given by the Stoke−Einstein equation:

$$D_0 = kT/6\pi\eta R_s \tag{1}$$

where k is Boltzmann's constant, T is the temperature, η is the solvent viscosity, and R_s is the Stokes−Einstein radius of the solute. The phenomena of the diffusion of solutes in the

(32) Kang, M. S.; Martin, C. R. *Langmuir* **2001**, *17*, 2753−2759.

(33) Craig, V. S. J.; Ninham, B. W.; Pashley, R. M. *J. Phys. Chem.* **1993**, *97*, 10192−10197.

(34) Maheswari, R.; Dhathathreyan, A. *J. Colloid Interface Sci.* **2004**, *275*, 270−276
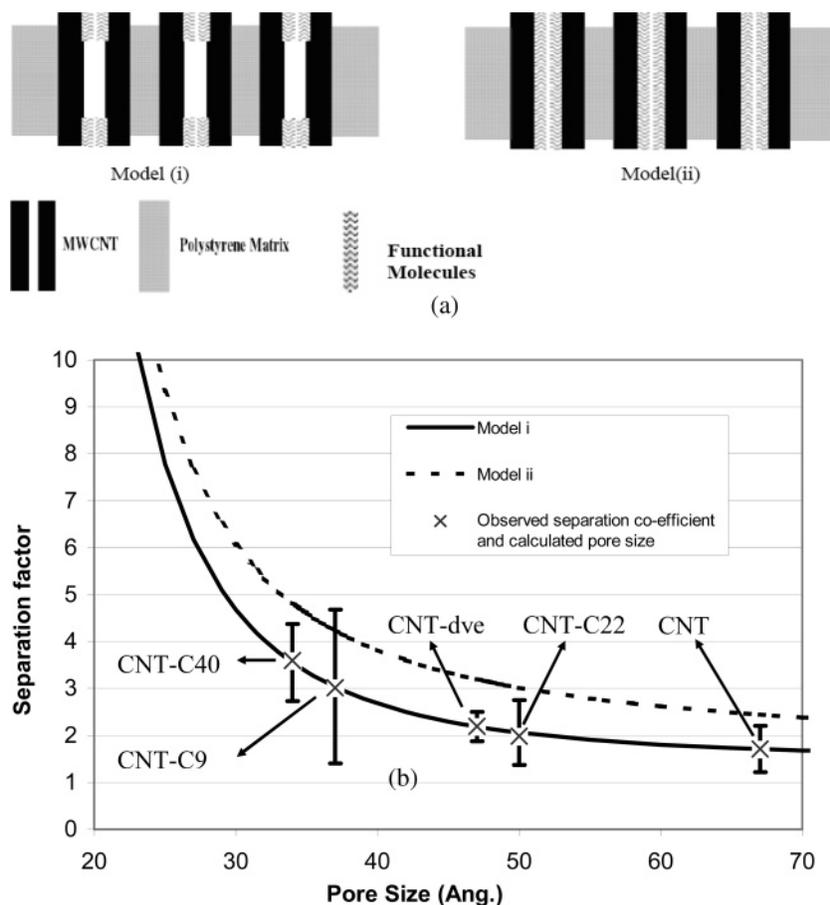
Figure 5. (a) Schematic and (b) separation factor (α) with error bars (at 90% confidence) versus pore size for (i) hindered diffusion at the entrance and exit to the nanotubes and (ii) hindered diffusion throughout the nanotube. Model (ii) predicts a higher α than model (i) due to a longer hindered diffusion path length.

constrained space of pores causes the molecular friction to exceed the value in the bulk, thereby decreasing the effective diffusivity in the pores. Two correction factors[35] are used to model the phenomena of hindered diffusion, both of which can be expressed as a function of the reduced pore diameter, λ, given by:

$$\lambda = \text{permeate molecule diameter/pore diameter} \quad (2)$$

Hindered diffusion becomes dominant when λ approaches 1; for $\lambda > 1$, solute exclusion occurs. For purely steric interactions between the solute and the pore wall, the hindered diffusivity, D_h, can be expressed by Renkin's equation[28] as

$$D_h = D_0(1 - \lambda)^2(1 - 2.104\lambda + 2.09\lambda^3 - 0.95\lambda^5) \quad (3)$$

It is of interest to compare experimental separation coefficients (α) to predictions of hindered diffusion at the CNT tip entrances in order to verify a "gatekeeper" transport limited mechanism

The models considered were as follows: (i) hindered diffusion only at distances $L_1/2$ at the two ends of the CNT and normal diffusion along the length L_2, so the total length of the nanotube is thus $L_1 + L_2$; (ii) hindered diffusion throughout the nanotube. Schematics for the two models are shown in Figure 5a. We assume steady-state conditions for this model. Since the cross-

(35) Deen, W. M. *AIChE. J.* **1987**, *33*, 1409−1425.

sectional area inside the nanotube is changing, $W = NA$ is constant, where W is the molar transport rate (mol/h), N is the molecular flux (mol/cm^{2}h), and A is the pore area (cm^2). We also assume that the concentration of a species changes along the nanotube, with C_1 (mol/cm^3) at the entrance and C_4 (mol/cm^3) at the exit, which are same as the feed and permeate concentration, respectively. C_2 (mol/cm^3) and C_3 (mol/cm^3) are the concentrations at the end of the first functional layer at the entrance and at the beginning of the second functional layer at the exit. The cross-sectional area of nonfunctionalized nanotube is A_0 (cm^2), and the area where hindered diffusion occurs is A_h (cm^2). These areas are given by

$$A_0 = \pi d_0^2/4; A_h = \pi d_p^2/4 \quad (4)$$

where d_0 is the diameter (Å) of the inner core of the nanotube and d_p is the pore diameter (Å) at the entrance and exit. Thus,

$$W = -D_h A_h(C_1 - C_2)/0.5L_1 = -D_0 A_0(C_2 - C_3)/L_2 = -D_h A_h(C_3 - C_4)/0.5L_1 \quad (5)$$

$$= -(C_1 - C_2)/(0.5L_1/D_h A_h) = -(C_2 - C_3)/(L_2/D_0 A_0) = -(C_3 - C_4)/(0.5L_1/D_h A_h)$$

$$= -(C_1 - C_4)/(L_1/D_h A_h + L_2/D_0 A_0)$$

For two different molecules, with bulk diffusivities $D_{0,1}$ and $D_{0,2}$, respectively, the following separation factor (α) is pro-

posed:

$$\alpha = (L_1/D_{h,2}A_h + L_2/D_{0,2}A_0)/(L_1/D_{h,1}A_h + L_2/D_{0,1}A_0) \quad (6)$$

This equation can be simplified for model (ii) in which $L_2 = 0$; thus

$$\alpha = D_{h,1}/D_{h,2} \quad (7)$$

For the probe molecules, ruthenium bipyridine is a spherical molecule with a diameter of about 11.8 Å. This agrees quite well with the Stoke−Einstein derived diameter of 12 Å. MV^{2+} is a cylindrical molecule with length 11 Å and breadth 3.3 Å. The equivalent spherical diameter for the molecule is about 5.2 Å. Diffusion studies in porous alumina[6] saw a flux reduction for MV^{2+} of 10^3 when pore size was reduced from 5.5 nm to 0.6 nm. Their data are remarkably consistent for an expected flux reduction of 1000. This is based on a factor of 83 (for reduction of pore size) and a factor of 13.8 (for reduction due to hindered diffusion) using the equivalent spherical diameter of MV^{2+} of 5.2 Å. Thus, reduced pore diameter for each species can be closely approximated as a function of d_p based on equivalent spherical diameter. The bulk diffusivity of Ru-(bipy)$_3$$^{2+}$ is 5.16×10^{-6} cm^2/s.[36] The bulk diffusivity[8] of MV^{2+} is 1.5 times that of Ru-(bipy)$_3$$^{2+}$ (i.e., $D_{0,1}/D_{0,2} = 1.5$).

Experiments were carried out to estimate the functional density and the length up to which the nanotube tips were oxidized. The carbon nanotube membrane was dissolved in toluene and centrifuged to remove the polymer. Thereafter, the nanotubes were functionalized with 2-aminoethanethiol using the same carbodiimide chemistry and decorated[37] with gold nanoparticles (10 nm diameter) by covalent linkage with the thiol group of 2-aminoethanethiol. By TEM the nanoparticle density was observed as the number of nanocrystalline Au (nc-Au) particles/length of CNT for 30 different CNTs of 10 μm length.[38] The Au nanoparticle density decreased from 526 particles/micron at the tips to negligible (<7 particles/micron) at a location 700 nm from the carbon nanotube tips. At the tips, the surface coverage of nc-Au was ∼52%. This is consistent with the previous argument that the functional molecules at the tip CNTs are not likely molecularly dense (packed). However, this Au nanoparticle decoration experiment is only a lower limit since several functional molecules (2-aminoethanethiol) may be attached to the same Au nanoparticle. The carbon nanotubes were also functionalized at each end a distance ∼7% of the total length of the nanotube. This is consistent with experimental observation of CNT tips slightly above the polystyrene matrix due to differing oxidation rates of CNT and polystyrene.[15] Though the exteriors of the CNTs were decorated with Au particles, here we assume that the same oxidation process occurred inside during functionalization with molecules. Thus, L_1 is ∼14% and L_2 is ∼86% of the total length of the nanotubes. The selectivity vs pore size (d_p) plots for the two models are shown in Figure 5b. Consistent pore sizes of the different membranes can be calculated from the first model and the experimentally observed separation factors. These calculated values are also shown in Table 1. Importantly, in the case of the as-oxidized (carboxlyate only functionality) membrane, model (i) gives a calculated pore size of 67 Å, which is consistent with microscopic characterization of MWCNT cores. Using model (ii), the calculated core diameter of as-oxidized carbon nanotubes is 20 nm. Furthermore, the functional molecules would not be physically long enough to give the observed higher separation coefficients as seen in the chemically modified membranes. The higher flux observed with anionic dye molecule supports this model of tip functionalization. If the CNT cores were lined with an attractive anionic charge we would expect a reduction in the flux of cations due to partitioning onto pore walls with a decrease in effective diffusion coefficients. This effect is commonly seen in ion exchange membranes.[39] A somewhat subtle point of model (i) is the assumption of bulk diffusivity D_o in the nonfunctionalized region of the CNT core. This would indicate that the permeate molecules have little interaction with the CNT wall since hindered diffusion is based largely on frictional interaction of the permeating molecule with the pore wall.[35] This would be expected from theoretical studies predicting that water molecules have a several Å gap with the CNT wall due to surface energy mismatch.[11] Polyethylene monomers diffusing in a CNT core are also predicted to keep a distance of about 4 Å from the CNT walls.[40] Other theoretical studies predict much higher diffusivities than those in other nanoporous materials[32,41,42] due to minimal frictional resistance between the inherently smooth potential energy surfaces of the graphitic CNT interiors. Implicit in our hindered diffusion model (with hindrance only at the entrances to CNT cores) is that increases in overall flux across the membrane due high diffusivities predicted inside CNT cores may be limited by the chemical interactions ("gatekeeper" functionality) at the tips of the CNT. The data and model shown here are self-consistent but are not definitive proof of the nature of conduction through the CNT due to the experimental uncertainty of the areal density and the conformation of functionalized "gate keeper" molecules.

4. Conclusions

Chemical functionalization at the entrance to CNT cores affects the selectivity of chemical transport across an aligned membrane structure. The CNT tips are modified using broadly applied carboimide chemistry which is confirmed by FTIR and electron microscopy of nc-Au decorated sites observations. Since the selectivity of transport is modified through chemical functionality, the observed flux through the CNT membrane cannot be through macroporous cracks in the polymer matrix. Additionally the lack of flow through membranes using CNTs that are blocked by iron catalyst particles indicates that the polystyrene polymer matrix is not rendered mesoporous by the fabrication steps. Increasing the length of the gatekeeper molecule at CNT core entrance is seen to improve size-based selectivity. However, longer aliphatic functional molecules have poor aqueous solvation resulting in reduced selectivity. This indicates the importance of functional molecular configuration.

(36) Martin, C. R.; Rubunstein, I.; Bard, A. J. *J. Electroanal. Chem.* **1983**, *151*, 267−271.
(37) Moghaddam, M. J.; Taylor, S.; Gao, M.; Huang, S. M.; Dai, L. M.; McCall, M. J. *Nano Lett.* **2004**, *4*, 89−93.
(38) Chopra, N.; Majumder, M.; Hinds, B. J. *Adv. Funct. Mater.* **2005**, *15*, 858−864.

(39) Miyoshi, H. *Sep. Sci. Technol.* **1999**, *34*, 231−241.
(40) Wei, C.; Srivastava, D. *Phys. Rev. Lett.* **2003**, *91*, 235901-1-4.
(41) Sokhan, P. S.; Davidson, N.; Quirke, N. *J. Chem. Phys.* **2002**, *117*, 8531−8539.
(42) Skoulidas, A. I.; Ackerman, D.; Johnson, J. K.; Sholl, D. *Phys. Rev. Lett.* **2002**, *89*, 185901-1-4.

Use of anionically charged dye molecules as gatekeepers dramatically improves cationic transport through the membrane due to Coloumbic attraction. A hindered diffusion model with lowered diffusivity near the entrances of CNT cores and with bulk diffusion along the length of CNTs was consistent with observed separation coefficients (α) as a function of chemical functionality. Thus the overall chemical flux through CNT membranes is largely limited by chemical interactions of functional molecules at the CNT core entrances.

JA043013B